

Theorems relating to port interchange in current mode CCII circuits

AHMED M. SOLIMAN†

The objective of this paper is to introduce new useful theorems relating to port interchange in current mode current conveyor circuits. Several applications of the theorems are given, among which a new current mode notch and all-pass filter with complex poles is generated from a known circuit with real axis poles, based on the interchange of the input and ground theorem. PSpice simulations are included.

1. Introduction

Most of the current conveyor (CCII) circuits that are proposed in the literature are based on similar available op.-amp. circuits. A theorem relating to op.-amp. to CCII circuits has been given (Soliman 1995). This theorem can lead to the generation of a wide class of CCII circuits from op.-amp. circuits.

It is well known that interchanging the input terminals of a stable op.-amp. circuit results in an unstable circuit; this is due to the finite gain bandwidth of the op.-amp. This property, however, does not exist in the CCII circuits. Therefore the coupling between the op.-amp. and CCII circuits should be removed, and an independent study on the CCII circuits should be initiated. This is one of the main objectives of this paper.

The current mode circuits considered in this paper employ two types of the CCII's. The first is the single-output CCII and the second is the two-output CCII. The symbolic representation of these CCII's is shown in Fig. 1, and their matrix equations are described below.

The single-output CCII is a three-port active building block which is described by the following matrix equation (Sedra and Smith 1970):

$$\begin{bmatrix} V_x \\ I_y \\ I_z \end{bmatrix} = \begin{bmatrix} 0 & 1 & 0 \\ 0 & 0 & 0 \\ K & 0 & 0 \end{bmatrix} \begin{bmatrix} I_x \\ V_y \\ V_z \end{bmatrix} \quad (1)$$

If $K = 1$ the CCII is defined as a CCII+; on the other hand, if $K = -1$ the CCII is defined as a CCII-.

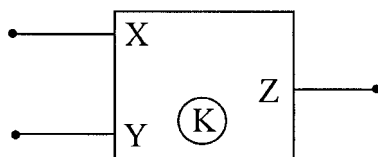
The two-output CCII is a four-port active building block which is defined by the following matrix equation:

$$\begin{bmatrix} V_x \\ I_y \\ I_{z1} \\ I_{z2} \end{bmatrix} = \begin{bmatrix} 0 & 1 & 0 & 0 \\ 0 & 0 & 0 & 0 \\ K & 0 & 0 & 0 \\ -K & 0 & 0 & 0 \end{bmatrix} \begin{bmatrix} I_x \\ V_y \\ V_{z1} \\ V_{z2} \end{bmatrix} \quad (2)$$

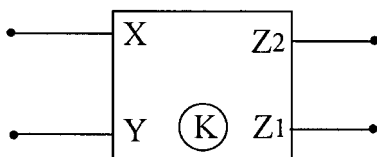
Most recently a novel CMOS realization of the two-output CCII has been reported (Elwan and Soliman 1996).

Received 4 June 1986; accepted 14 October 1996

†Electronics and Communications Engineering Department, Cairo University, Giza, Egypt.



(a)



(b)

Figure 1. The symbolic representation of: (a) the single-output CCII; (b) the two-output CCII.

The current mode circuits considered in this paper are divided into two classes. The first circuits considered are those without feedback, and they are given in §§ 2 and 3. The second circuits employ feedback, and they will be discussed in § 4.

2. The interchange of the X and Y ports of the CCII

The first basic configuration considered in this section is shown in Fig. 2 (a), which represents a current mode circuit with a transfer function $T_1(s)$, where N is a three-port RC network with no ground terminal. A very useful theorem is now given based on this generalized configuration.

Theorem 1: *Interchanging the X and Y ports of the CCII circuit shown in Fig. 2(a) results in the circuit shown in Fig. 2(b), whose transfer function T_2 is related to T_1 by the following equation:*

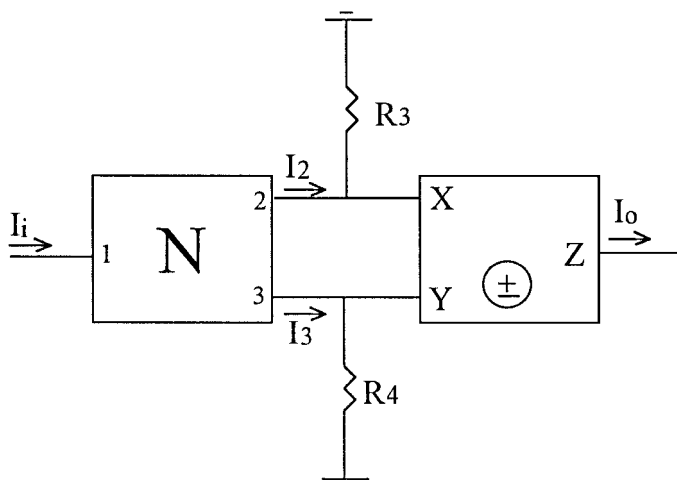
$$T_2 = -\frac{R_3}{R_4} T_1 \quad (3)$$

Proof: The voltage-conveying property of the CCII from port Y to port X implies that $V_2 = V_3$; thus the currents I_2 and I_3 in the circuit of Fig. 2(a) are the same as those in the circuit of Fig. 2(b). By direct analysis, the transfer functions for the two circuits are given, respectively, by

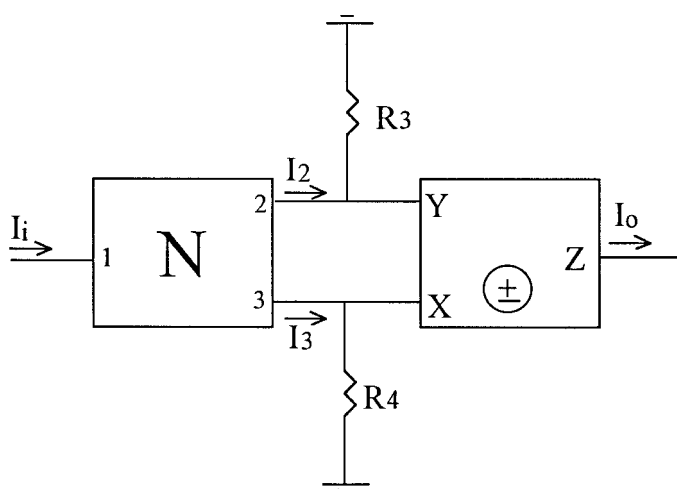
$$T_1 = \mp \left(T_{21} - \frac{R_4}{R_3} T_{31} \right) \quad (4)$$

$$T_2 = \pm \left(\frac{R_3}{R_4} T_{21} - T_{31} \right) \quad (5)$$

where



(a)



(b)

Figure 2. The two generalized CCII configurations related by the X and Y ports interchange theorem.

$$T_{21} = \frac{I_2}{I_i} \quad \text{and} \quad T_{31} = \frac{I_3}{I_i} \tag{6}$$

The upper sign applies to the CCII+ and the lower sign applies to the CCII- .

The proof of the theorem follows directly by comparing (4) and (5).

This theorem can be used to generate new current mode circuits from known circuits.

As an example, consider the notch filter which is obtained by using the network N shown in Fig. 3(a) with the configuration of Fig. 2(b) (Chang 1991), where

$$Y_1 = \frac{sC_1}{sC_1R_1 + 1}, \quad Y_2 = sC_2 + \frac{1}{R_2} \quad (7)$$

An alternative notch filter can be obtained using the same network N with the configuration of Fig. 2(a). The transfer function in this case, assuming that a CCII+ is used, is given by

$$T_1(s) = \frac{R_4}{R_3} \frac{s^2 C_1 C_2 R_1 R_2 - s \left(C_1 R_2 \frac{R_3}{R_4} - C_1 R_1 - C_2 R_2 \right) + 1}{s^2 C_1 C_2 R_1 R_2 + s(C_1 R_2 + C_1 R_1 + C_2 R_2) + 1} \quad (8)$$

The necessary condition for a notch response is

$$\frac{R_3}{R_4} = \frac{R_1}{R_2} + \frac{C_2}{C_1} \quad (9)$$

Thus a unity gain notch response can be obtained by taking

$$C_1 = 2C_2, \quad R_2 = 2R_1 \quad \text{and} \quad R_4 = R_3 \quad (10)$$

Fig. 4 shows the PSpice simulation of the magnitude response of this notch filter with $C_1 = 2$ nF, $C_2 = 1$ nF, $R_1 = 10$ k Ω , $R_2 = 20$ k Ω and $R_3 = R_4 = 10$ k Ω . The simulation is based on use of the analogue device AD844 biased with ± 12 V and using $I_i = 10$ mA. The output current I_0 is measured in a 1 k Ω load resistor connected between the Z terminal and the ground. From the simulation it is seen that f_0 is very close to its theoretical value of 7.96 kHz.

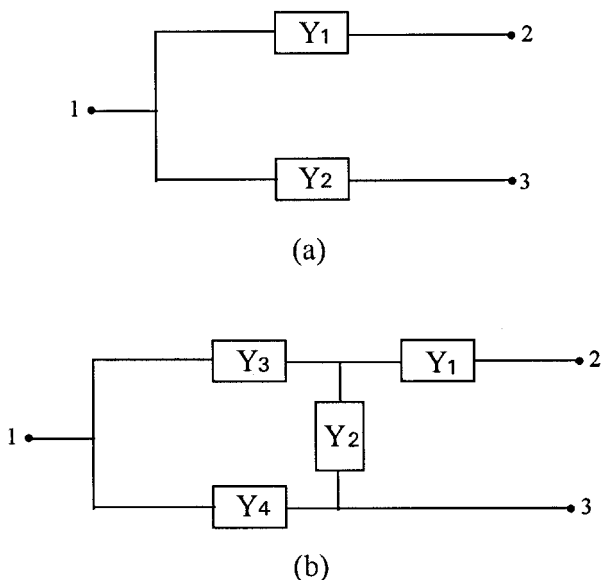


Figure 3. The two generalized configurations for the passive network N .

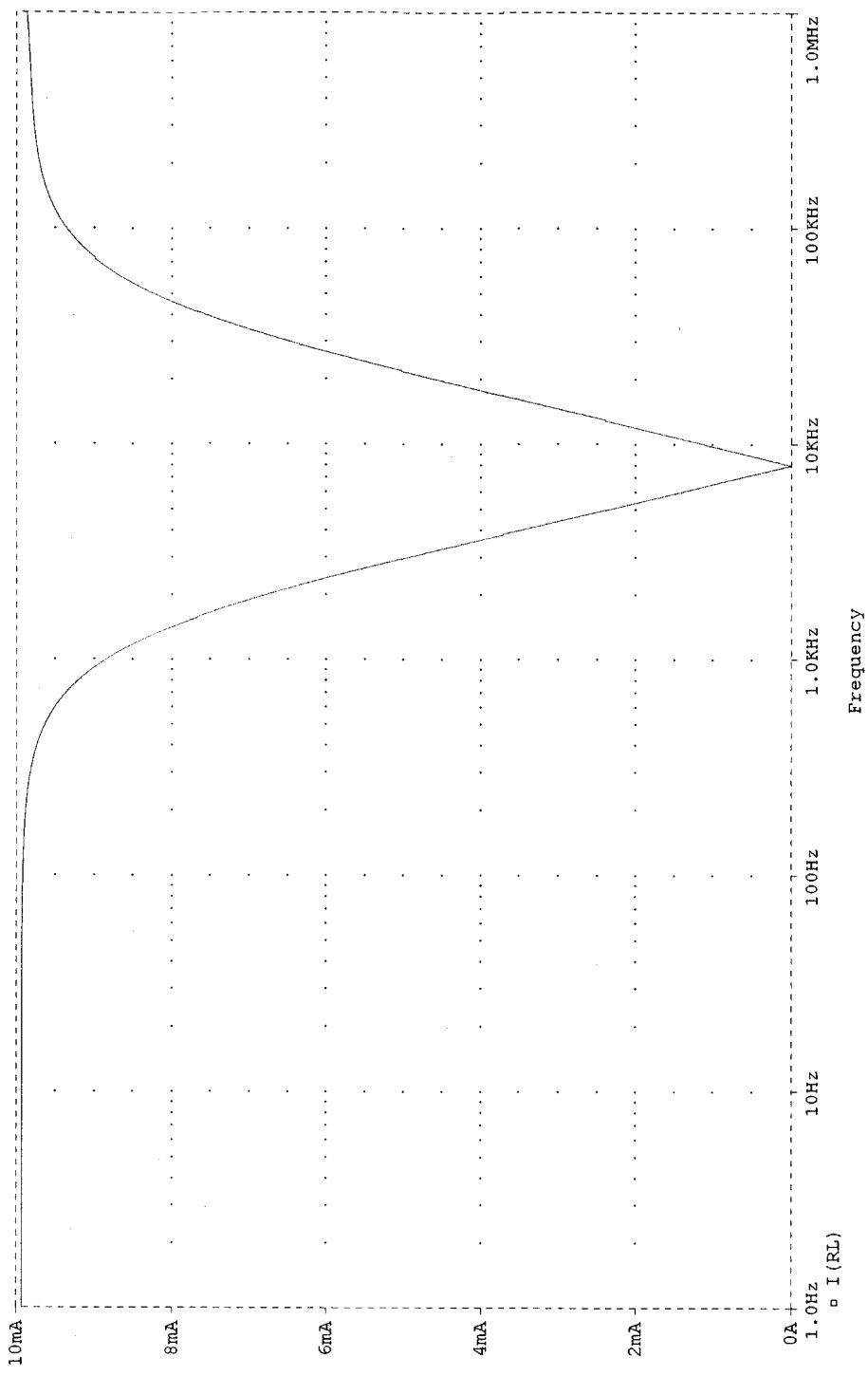


Figure 4. PSpice simulation of the magnitude response of the new notch filter based on the configuration shown in Fig. 2(a).

When a CCII+ is used with the circuit of Fig. 2(a), the special case $R_3 = R_4$ becomes of interest, because I_0 is simplified to

$$I_0 = I_3 - I_2 \quad (11)$$

The above equation can be realized by removing the two equal resistors and connecting port Y of the CCII+ directly to port Z , as shown in Fig. 5(a).

Similarly, the circuit of Fig. 2(b) can be simplified to that shown in Fig. 5(b) and Theorem 1 is modified as given by the following corollary.

Corollary 1: *Interchanging ports 2 and 3 of the network N in the circuit of Fig. 5(a) results in the circuit of Fig. 5(b) whose transfer function T_2 is given by*

$$T_2 = -T_1 \quad (12)$$

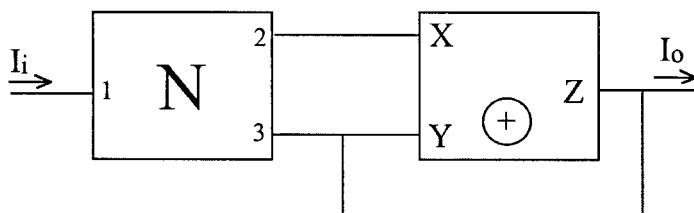
The configurations of Fig. 5 are very useful in generating minimum R and C first-order all-pass and second-order notch filters, as discussed in the following subsections.

2.1. First-order canonic all-pass filters

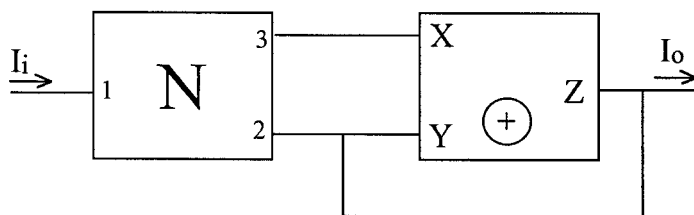
Using the circuit of Fig. 3(a) with the configuration of Fig. 5(a) results in the following current transfer function:

$$T(s) = \frac{Y_2 - Y_1}{Y_2 + Y_1} \quad (13)$$

Taking $Y_1 = sC$ and $Y_2 = 1/R$, results in the circuit shown in Fig. 6(a), whose transfer function is



(a)



(b)

Figure 5. The CCII+ simplified configurations obtained from Fig. 2 for the special case $R_3 = R_4$.

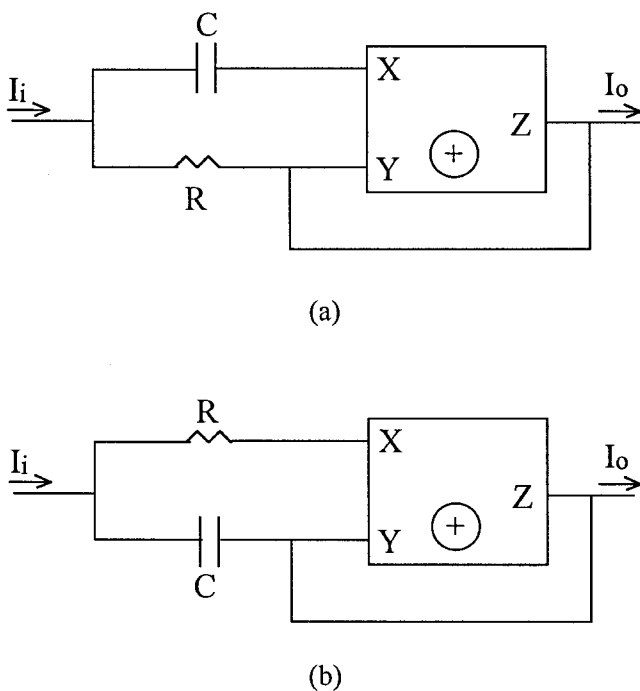


Figure 6. The minimal realizations of the all-pass current mode filters.

$$T(s) = \frac{1 - sCR}{1 + sCR} \quad (14)$$

The above equation represents a first-order all-pass with an adjustable phase from 0 to -180° .

Applying Corollary 1 to the circuit of Fig. 6(a) results in the all-pass of Fig. 6(b) whose phase is adjustable from 180° to 0.

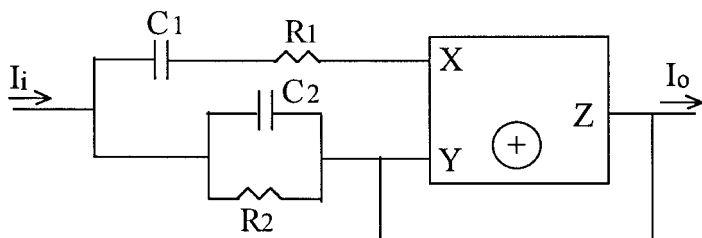
It is worth noting that the minimum R and C all-pass circuits of Fig. 6 employ the CCII as a negative impedance converter (NIC), and for a finite load they are different from the circuits that employ the CCII as a current follower which were given by Soliman (1972) in a generalized form of a first-order transfer function and re-published by Liu *et al.* (1995).

2.2. Canonic notch filters

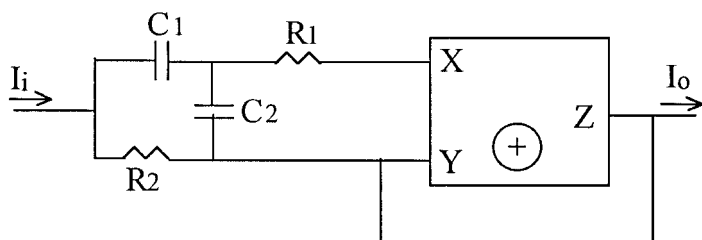
In this section six new minimal realizations of current mode notch filter circuits are described. The circuits given in Fig. 7 are based on the configuration of Fig. 5(a), and those given in Fig. 8 are based on the configuration of Fig. 5(b).

Figure 7(a) represents the non-inverting unity gain notch filter based on the network N of Fig. 3(a) with Y_1 and Y_2 taken as given by (7). The necessary condition for a notch response is given by

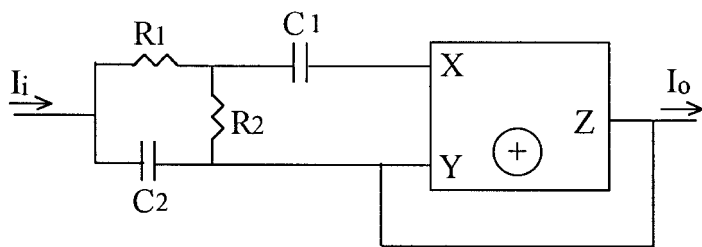
$$\frac{R_1}{R_2} + \frac{C_2}{C_1} = 1 \quad (15)$$



(a)



(b)



(c)

Figure 7. Three alternative minimal realizations of the non-inverting current mode notch filters.

The notch filters given in Figs. 7(b) and (c) are related to each other by the $RC : CR$ transformation and are based on the network of Fig. 3(b). The notch conditions are given, respectively, by

$$\frac{R_2}{R_1} = 1 + \frac{C_2}{C_1} \quad (16)$$

$$\frac{C_1}{C_2} = 1 + \frac{R_1}{R_2} \quad (17)$$

Applying Corollary 1 to the non-inverting notch filters of Fig. 7 results in the three inverting notch filters shown in Fig. 8.

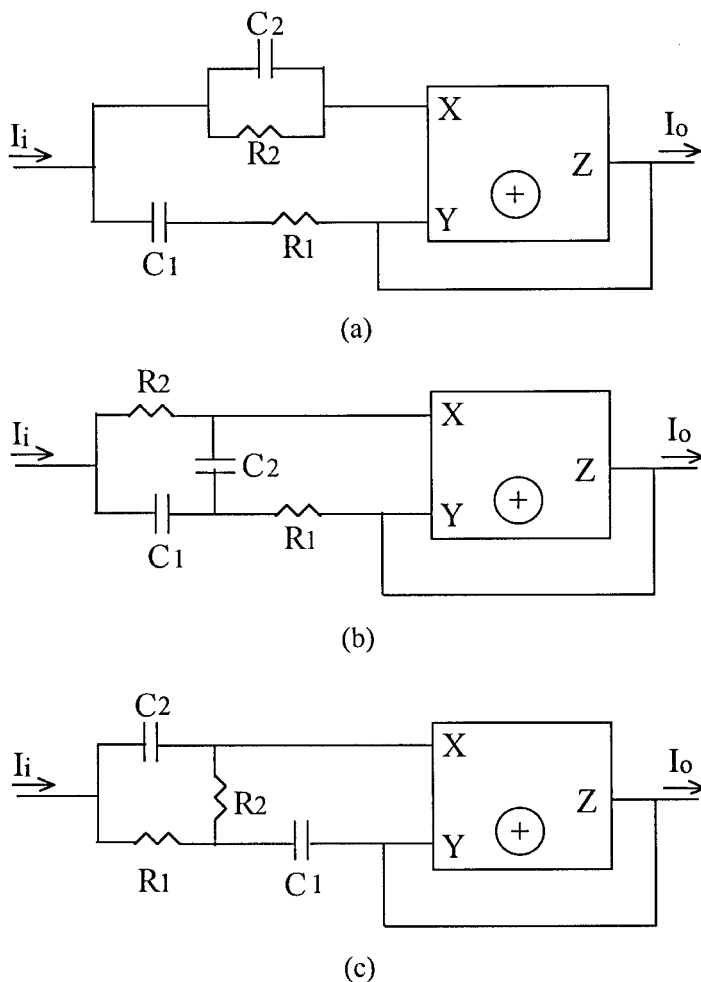


Figure 8. Three alternative minimal realizations of the inverting current mode notch filters.

Figure 9 shows the PSpice simulation of the notch filter of Fig. 8(c) with $C_1 = 2$ nF, $C_2 = 1$ nF, $R_1 = R_2 = 10$ k Ω , $I_i = 10$ mA and $R_L = 1$ k Ω . From the simulation it is seen that f_0 is very close to its theoretical value of 11.25 kHz.

3. The interchange of the input and ground

The complementary network theorem (Hilberman 1973), which is based on the interchange of the input and ground, is a very powerful theorem in voltage mode circuits. In this section an extension of this theorem to the current mode circuits employing the CCII is given.

Theorem 2: *Interchanging the input and the ground of the CCII circuit shown in Fig. 10(a), whose transfer function is T_1 results in the circuit shown in Fig. 10 (b), whose transfer function T_2 is related to T_1 by the following equation:*

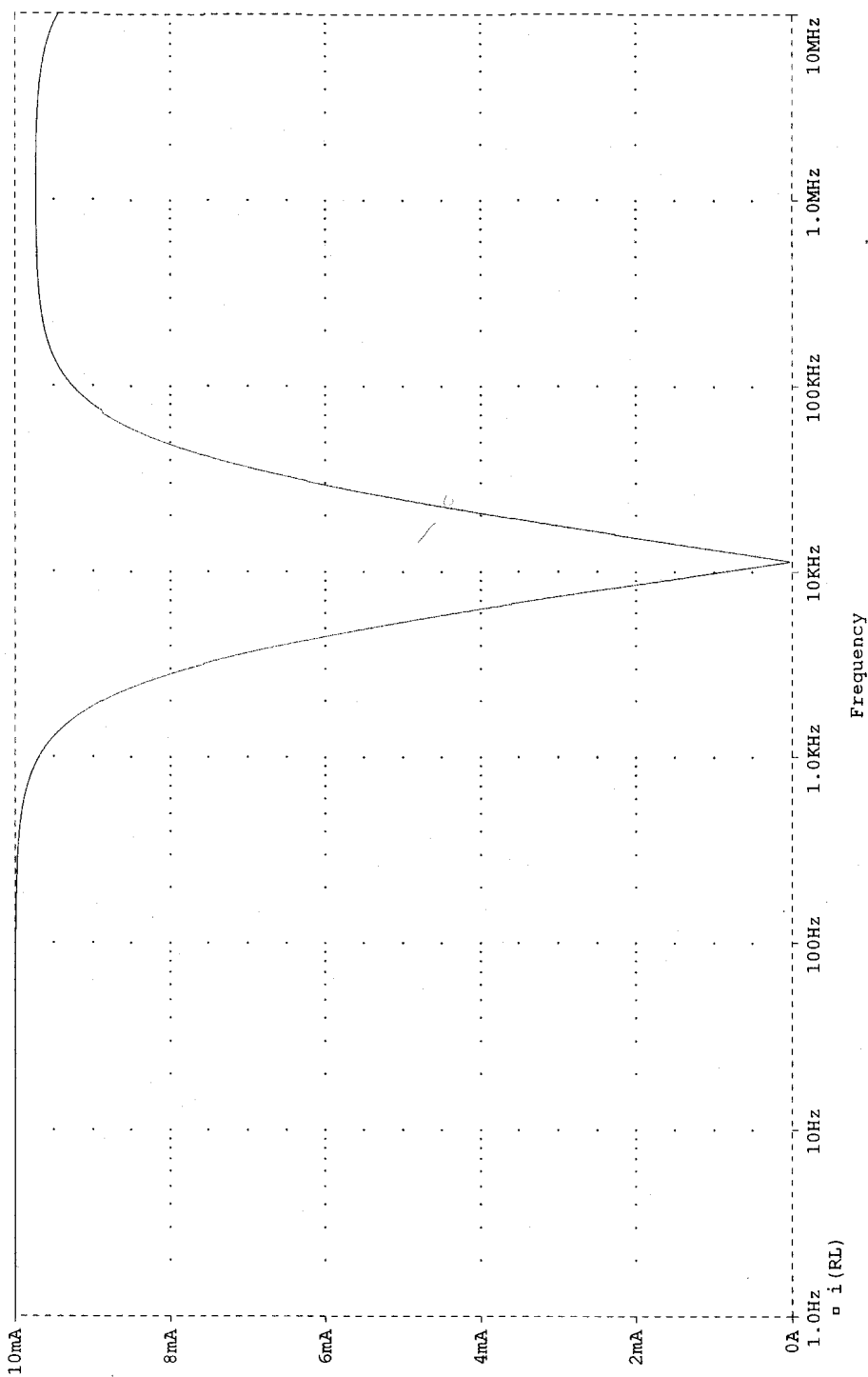
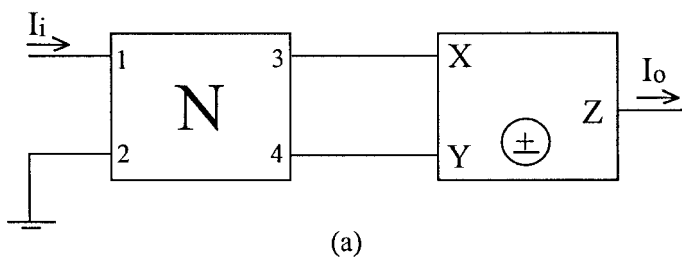
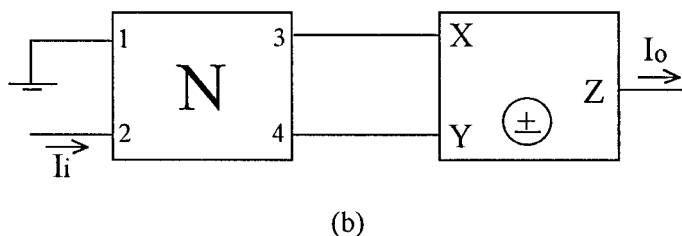


Figure 9. PSpice simulation of the magnitude response of the new notch filter based on the configuration shown in Fig. 8(c).



(a)



(b)

Figure 10. The two generalized CCII configurations related by the interchange of the input and ground theorem.

$$\frac{1}{T_1} + \frac{1}{T_2} = \mp 1 \tag{18}$$

The upper sign applies to the CCII+ and the lower sign applies to the CCII- .

The proof of this theorem is a straightforward generalization of the proof given in § 3.1, and it is not included to limit the length of the paper.

As a first application of this theorem, consider the notch filter which is based on using the network *N* of Fig. 3(a) with the generalized configuration of Fig. 2(a) and whose transfer function is given by (8). Interchanging the input and ground results in the grounded-*C* notch filter (Chang 1991b), which is also limited to real axis poles.

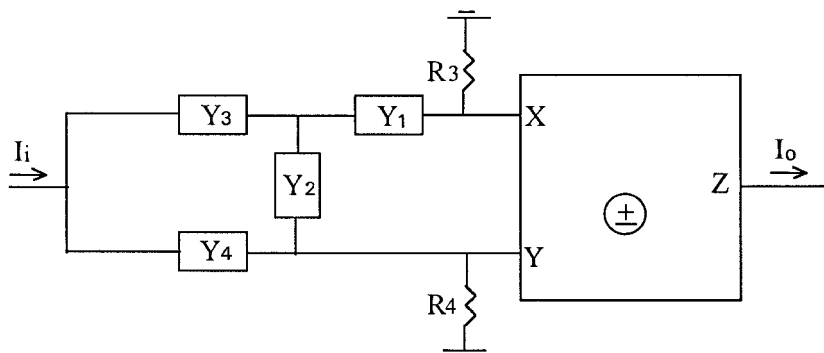
A very important application of the theorem in realizing a new current mode notch filter with complex poles is given next.

Consider the circuit shown in Fig. 11(a) which is based on using the network *N* of Fig. 3(b) with the generalized configuration of Fig. 2(a). The transfer function of this circuit is given by

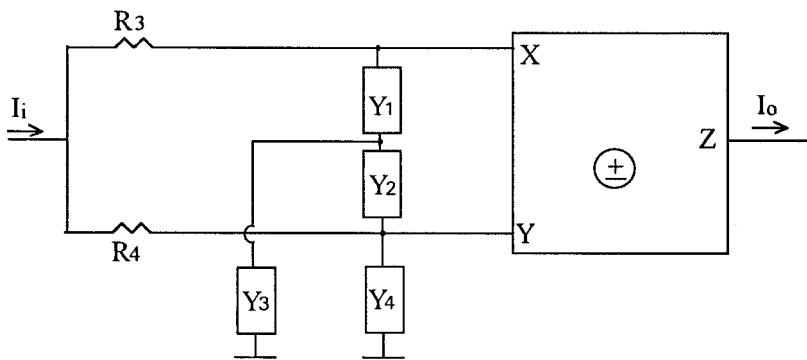
$$T_1(s) = \pm \frac{R_4}{R_3} \frac{Y_4(Y_1 + Y_2 + Y_3) + Y_2 Y_3 - \frac{R_3}{R_4} Y_1 Y_3}{Y_4(Y_1 + Y_2 + Y_3) + Y_2 Y_3 + Y_1 Y_3} \tag{19}$$

This circuit realizes all-pass and notch responses with design equations as given in the Table (Soliman 1996); it is limited, however, to real axis poles.

Applying Theorem 2 to this current results in the new current mode circuit shown in Fig. 11(b) which is capable of realizing complex poles. The transfer function is



(a)



(b)

Figure 11. (a) The current mode notch (all-pass) filter with real axis poles; (b) the new current mode notch (all-pass) filter with complex poles.

$$T_2(s) = \mp \frac{R_4}{R_3 + R_4} \frac{Y_4(Y_1 + Y_2 + Y_3) + Y_2 Y_3 - \frac{R_3}{R_4} Y_1 Y_3}{Y_4(Y_1 + Y_2 + Y_3) + Y_2 Y_3} \quad (20)$$

Figure 12 shows the PSpice simulation of the magnitude response using realization I with $R_1 = 1 \text{ k}\Omega$, $R_2 = 25 \text{ k}\Omega$, $C_1 = C_2 = 1 \text{ nF}$, $R_3 = 2 \text{ k}\Omega$ and $R_4 = 25 \text{ k}\Omega$, which realizes a notch response with $Q = 2.5$ and $f_0 = 31.83 \text{ kHz}$. The simulations are based on using the AD844, and an input current of 10 mA . The output current is measured in $100 \text{ }\Omega$ load resistor connected between port Z and ground. From the simulation results it is seen that $f_0 = 31.81 \text{ kHz}$, which is very close to its theoretical value.

3.1. The current buffer-based circuits

The special case when port Y is grounded, that is the CCII acts as a current buffer is of interest, and it leads to the generation of a well-known current mode bandpass filter, as discussed in an example.

Circuit	Design equations								Gain factor
	Realization	Y_1	Y_2	Y_3	Y_4	Notch	All-pass		
Fig. 11(a)	I	$\frac{1}{R_1}$	SC_2	SC_1	$\frac{1}{R_2}$	$\frac{R_3}{R_4} = \frac{R_1}{R_2} \left(\frac{C_2}{1 + C_1} \right)$	$\frac{R_3}{R_4} = 1 + 2 \frac{R_1}{R_2} \left(\frac{C_2}{1 + C_1} \right)$	$\begin{bmatrix} \frac{R_4}{R_3} \\ \pm \end{bmatrix}$	
	II	SC_1	$\frac{1}{R_2}$	$\frac{1}{R_1}$	SC_2	$\frac{R_3}{R_4} = \frac{C_2}{C_1} \left(\frac{R_1}{1 + R_2} \right)$	$\frac{R_3}{R_4} = 1 + 2 \frac{C_2}{C_1} \left(\frac{R_1}{1 + R_2} \right)$		
Fig. 11(b)	I	$\frac{1}{R_1}$	SC_2	SC_1	$\frac{1}{R_2}$	$\frac{R_3}{R_4} = \frac{R_1}{R_2} \left(\frac{C_2}{1 + C_1} \right)$	$\frac{R_3}{R_4} = 2 \frac{R_1}{R_2} \left(\frac{C_2}{1 + C_1} \right)$	$\begin{bmatrix} \frac{R_4}{R_3 + R_4} \\ \mp \end{bmatrix}$	
	II	SC_1	$\frac{1}{R_2}$	$\frac{1}{R_1}$	SC_2	$\frac{R_3}{R_4} = \frac{C_2}{C_1} \left(\frac{R_1}{1 + R_2} \right)$	$\frac{R_3}{R_4} = 2 \frac{C_2}{C_1} \left(\frac{R_1}{1 + R_2} \right)$		

The design equations and the gain factor for the circuits of Figs 11(a) and (b)

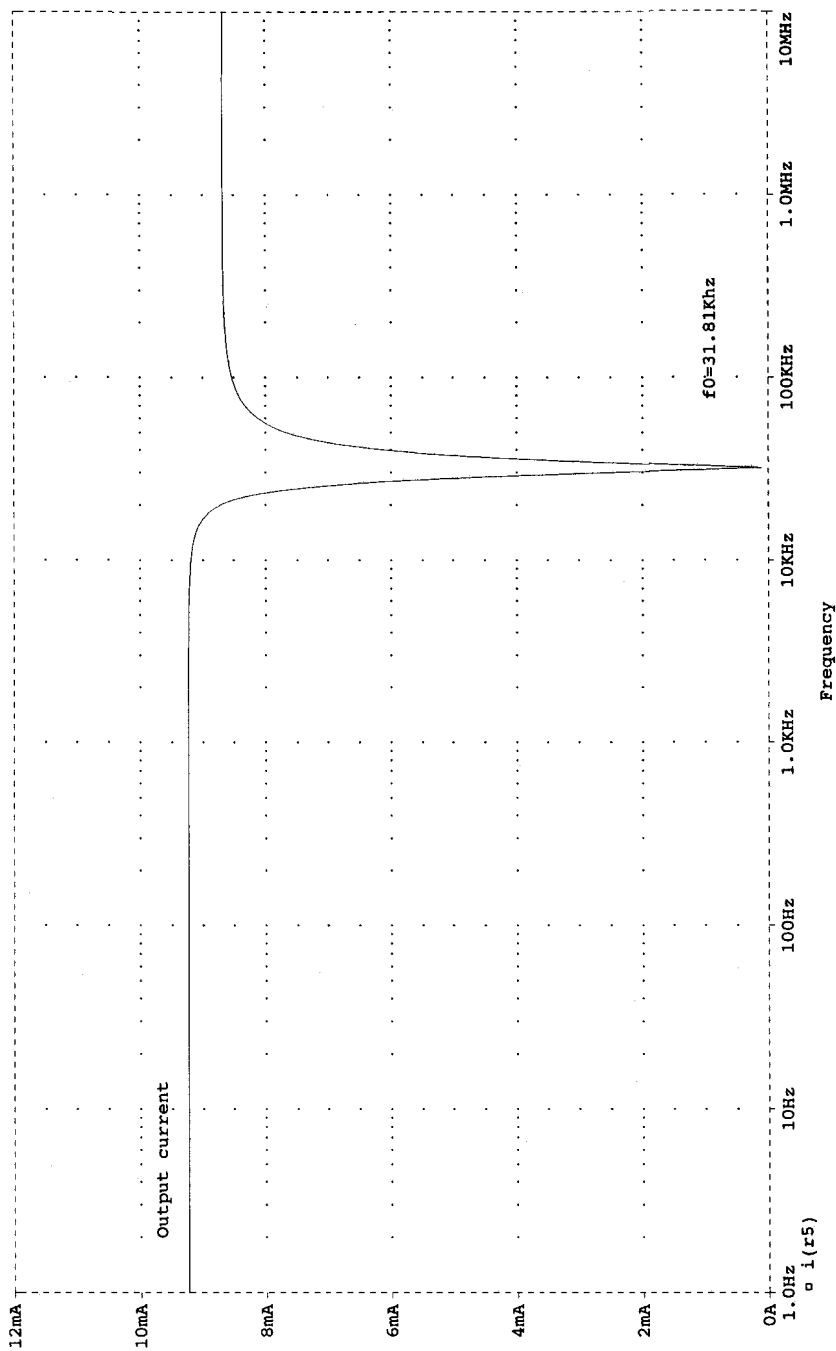


Figure 12. PSpice simulation of the magnitude response of the new notch filter based on the configuration shown in Fig. 11(b).

Corollary 2: The transfer function T_1 of the current buffer based circuit shown in Fig. 13(a) is related to the transfer function T_2 of the CCII based circuit shown in Fig. 13(b) by (18).

The proof is given for the case of a current buffer realized using a CCII+ , (the case of a CCII- differs only in the sign).

Let the y parameters of the reciprocal network N be represented by

$$y_{ij} \quad (i, j = 1, 2, 3)$$

For the circuit of Fig. 13(a), as $V_2 = V_3 = 0$, thus

$$I_i = I_1 = y_{11} V_1, \quad I_0 = I_3 = y_{31} V_1 \quad (21)$$

thus

$$T_1 = \frac{y_{31}}{y_{11}} \quad (22)$$

For the circuit of Fig. 13(b), as $V_1 = 0$ and $V_2 = V_3$,

$$I_i = I_2 = (y_{22} + y_{23}) V_2, \quad I_0 = I_3 = (y_{32} + y_{33}) V_2 \quad (23)$$

thus

$$T_2 = \frac{y_{32} + y_{33}}{y_{22} + y_{23}} = \frac{-y_{31}}{-y_{21}} \quad (24)$$

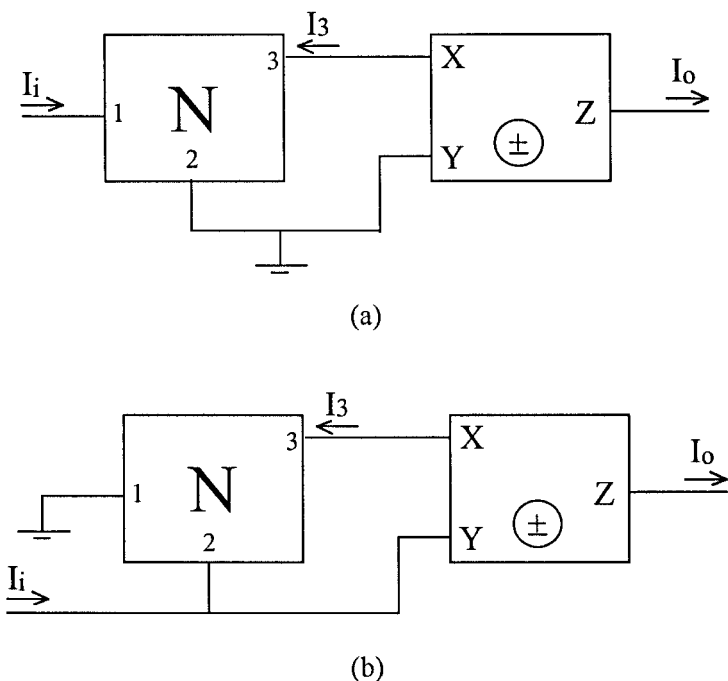


Figure 13. (a) The generalized configuration with the CCII acts as a current buffer; (b) The configuration obtained from Fig. 13(a) by interchanging the input and ground.

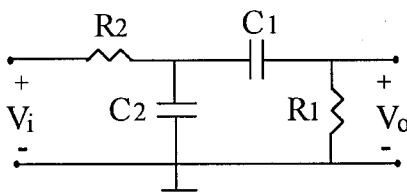
The second equality is based on the indefinite or the floating point matrix equations (Ghausi 1965).

From (22) and (24)

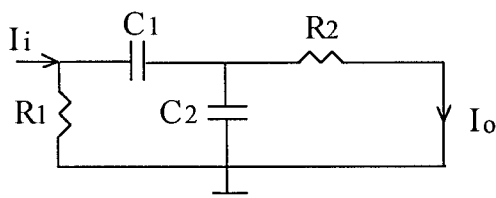
$$\frac{1}{T_1} + \frac{1}{T_2} = \frac{y_{11}}{y_{31}} + \frac{y_{21}}{y_{31}} = \frac{-y_{31}}{y_{31}} = -1 \quad (25)$$

This proves the corollary for the CCII+ case.

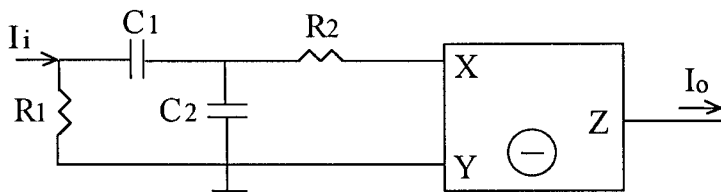
Example: Consider the well-known passive *RC* bandpass filter shown in Fig. 14(a), whose transfer function is



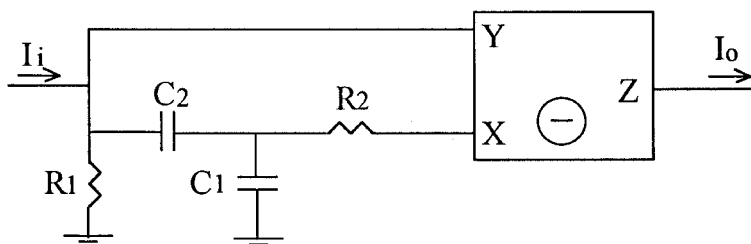
(a)



(b)



(c)



(d)

Figure 14. The three steps showing the generation of the current mode bandpass filter from the passive *RC* bandpass filter.

$$T_1(s) = \frac{sC_1 R_1}{s^2 C_1 C_2 R_1 R_2 + s(C_1 R_2 + C_1 R_1 + C_2 R_2) + 1} \quad (26)$$

Using the adjoint network theorem (Roberts and Sedra 1992) the current mode circuit shown in Fig. 14(b) is obtained, whose transfer function is the same as given by (26).

In order to use the current I_0 a current follower (realized using a CCII-) is added to the circuit as shown in Fig. 14(c).

Apply Corollary 2 to this circuit, the current mode bandpass filter shown in Fig. 14(d) is obtained (Liu *et al.* 1990), whose transfer function is given by

$$T_2(s) = \frac{-sC_1 R_1}{s^2 C_1 C_2 R_1 R_2 + s(C_1 R_2 + C_2 R_2) + 1} \quad (27)$$

4. Current mode circuits with feedback

In this section a theorem is given, based on the interchange of the excitation port in CCII circuits employing feedback. An application of the theorem in realizing a new current mode bandpass filter is given.

Consider the CCII circuit shown in Fig. 15(a) which is generated from the two-amplifier circuit (Ghausi and Laker 1981) using the adjoint network theorem and taking the amplifiers gains = ± 1 , which can easily be realized by current buffers with $K_i = \pm 1$ ($i = 1, 2$).

The transfer function for this circuit is given by

$$T_1 = \frac{K_1 K_2 Y_2 Y_3}{Y_1 Y_4 + Y_1 Y_3 + Y_2 Y_3 + Y_2 Y_4 (1 - K_1 K_2)} \quad (28)$$

Taking

$$Y_1 = sC_1, \quad Y_2 = \frac{1}{R_1}, \quad Y_3 = \frac{1}{R_2}, \quad Y_4 = sC_2 \quad \text{and} \quad K_1 K_2 = 1 \quad (29)$$

The circuit realizes a lowpass response with

$$\omega_0 = \frac{1}{(C_1 C_2 R_1 R_2)^{1/2}} \quad \text{and} \quad Q = \left(\frac{C_2 R_2}{C_1 R_1} \right)^{1/2} \quad (30)$$

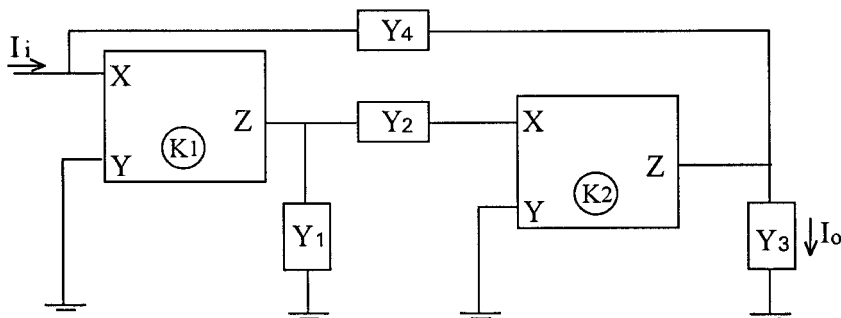
Although a bandpass response can be realized using this configuration by interchanging R_1 and C_1 and taking $K_1 K_2 = -1$, it is of limited practicality because the maximum realizable Q is 0.707.

The excitation port interchange theorem given in this section enables the modification of this circuit to realize a practical bandpass response as explained next.

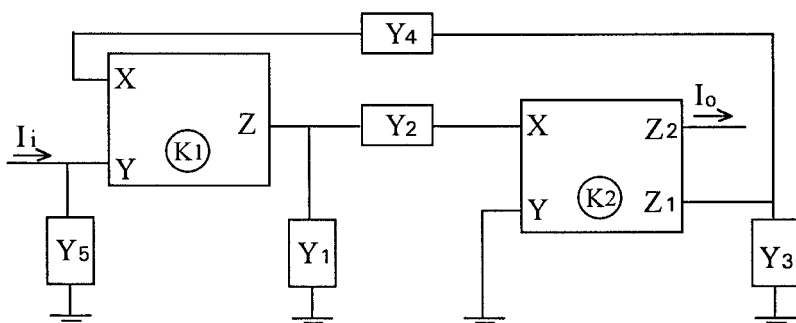
Theorem 3: *The transfer function T_2 of the CCII circuit shown in Fig. 15(b) which is generated from the circuit of Fig. 15(a) by interchanging the excitation port, and using a two-output CCII in place of the single-output CCII, is related to T_1 by the following equation:*

$$T_2 = \frac{Y_4}{Y_5} T_1 \quad (31)$$

The proof of this theorem is straightforward, thus it is not included.



(a)



(b)

Figure 15. The two-CCII configurations related by the excitation port interchange theorem.

Applying the above theorem to (28), the transfer function T_2 is

$$T_2 = \frac{K_1 K_2 \frac{Y_2 Y_3 Y_4}{Y_5}}{Y_1 Y_4 + Y_1 Y_3 + Y_2 Y_3 + Y_2 Y_4 (1 - K_1 K_2)} \quad (32)$$

Taking $Y_5 = 1/R_3$, and the remaining circuit parameters as given by (29); the transfer function is simplified to

$$T_2(s) = \frac{s C_2 R_3}{s^2 C_1 C_2 R_1 R_2 + s C_1 R_1 + 1} \quad (33)$$

which realizes a non-inverting bandpass response with the same ω_0 and Q as given by (30), and a centre frequency gain equals to $C_2 R_3 / C_1 R_1$. Fig. 16 shows the PSpice simulation of the magnitude response of this bandpass filter designed for $Q = 3$ and $f_0 = 53.05$ kHz, by taking $C_1 = 1$ nF, $C_2 = 3$ nF, $R_1 = 1$ k Ω , $R_2 = 3$ k Ω , $R_3 = 1$ k Ω and $I_i = 1$ mA. I_0 is measured in a 1 k Ω load resistor. The simulation is based on using the Elwan-Soliman, CMOS - CCIIs (1996). It is seen that the simulation results are in close agreement with their theoretical values.

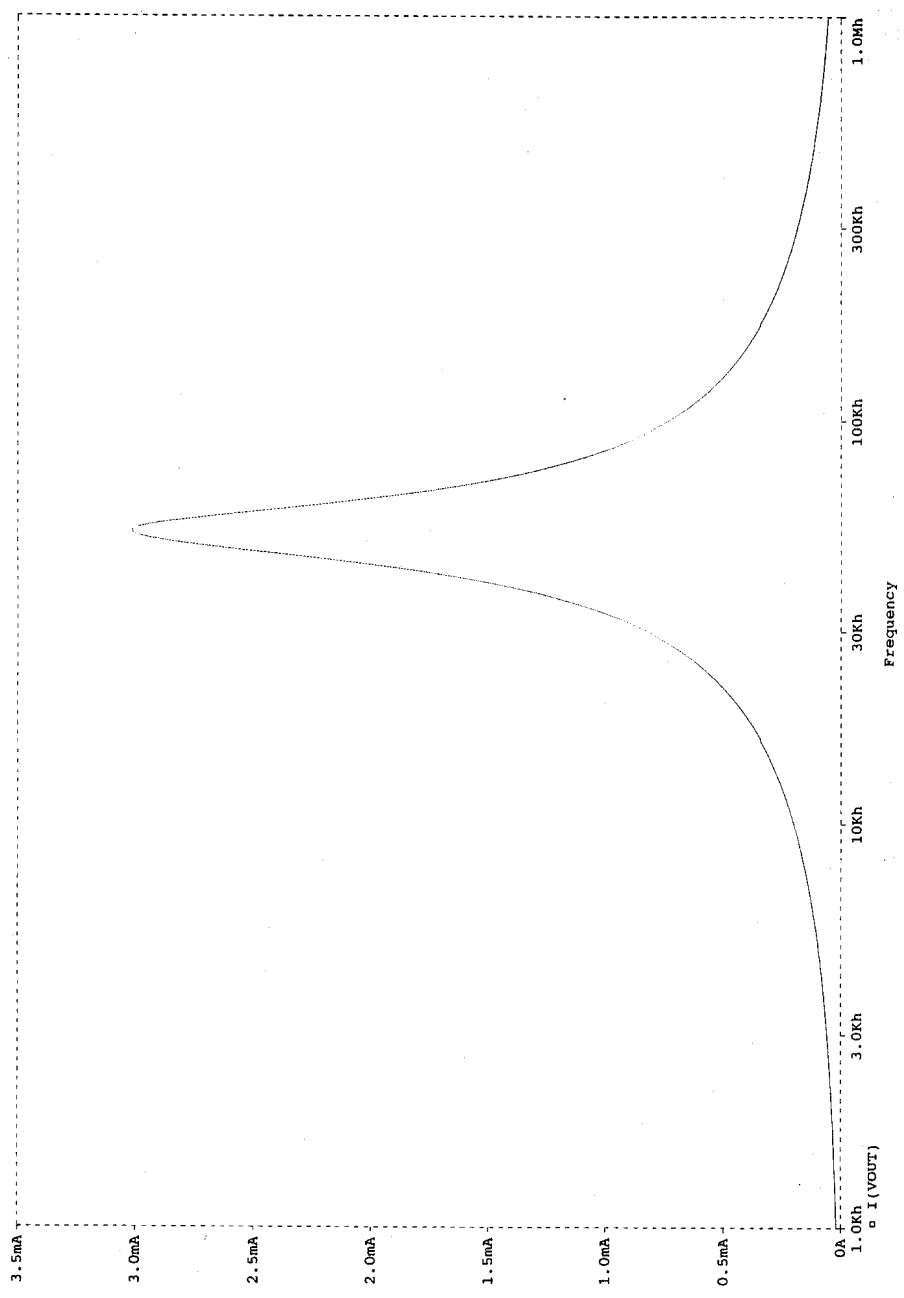


Figure 16. PSpice simulation of the magnitude response of the bandpass filter based on the configuration shown in Fig. 15(b).

5. Conclusion

Three useful theorems that relate to port interchange in current mode CCII circuits are given. The first theorem deals with the interchange of the X and Y ports of CCII circuits without feedback. New minimal realizations of all-pass and notch filters are given. A new current mode notch filter with complex poles is generated from a known notch filter with real axis poles using Theorem 2. The third theorem deals with CCII circuits with feedback. A new current mode bandpass filter is generated, based on the application of this theorem to a lowpass current mode circuit. PSpice simulation results are included.

REFERENCES

- CHANG, C. M., 1991 a, **Universal active current filters** using single second generation current conveyor. *Electronics Letters*, **27**, 1614–1617; 1991 b, Current mode allpass/notch and bandpass filter using single CCII. *Ibid.*, **27**, 1812–1813.
- ELWAN, H. O., and SOLIMAN, A. M., 1996, A novel CMOS current conveyor realization with an electronically tunable current mode filter suitable for VLSI. *IEEE Transactions on Circuits and Systems*, II, **43**, 663–670.
- GHAUSI, M. S., 1965, *Principles and Design of Linear Active Circuits* (New York: McGraw-Hill), pp. 56–62.
- GHAUSI, M. S., and LAKER, K. R., 1981, *Modern Filter Design, Active RC and Switched Capacitor* (Englewood Cliffs, NJ: Prentice Hall), pp. 212–215.
- HILBERMAN, D., 1973, Input and ground as complements in active filters. *IEEE Transactions on Circuit Theory*, **20**, 540–547.
- LIU, S. I., TSAO, H. W., and WU, J., 1990, Cascadable current-mode single CCII biquads. *Electronics Letters*, **26**, 2005–2006.
- LIU, S. I., CHEN, J. J., and HWANG, Y. S., 1995, New current mode biquad filters using current followers. *IEEE Transaction Circuits and Systems*, **42**, 380–383.
- ROBERTS, G. W., and SEDRA, A. S., 1992, A general class of current amplifier-based biquadratic filter circuits. *IEEE Transactions on Circuits and Systems*, **39**, 257–263.
- SEDRA, A., and SMITH, K. C., 1970, A second generation current conveyor and its applications. *IEEE Transactions on Circuit Theory*, **17**, 132–134.
- SOLIMAN, A. M., 1972, Active RC realization of current transfer functions using voltage generalized immittance converters. *International Journal of Electronics*, **33**, 273–280; 1995, Theorem relating a class of op-amp and current conveyor circuits. *Ibid.*, **79**, 53–61; 1996, New current mode notch and all-pass circuits using the current conveyor. *AEÜ*, **50**, 224–226.